The Astrophysical Journal Letters, 946:L49 (6pp), 2023 April 1 https://doi.org/10.3847/2041-8213/acc650

Cosmological-model-independent Determination of Hubble Constant from Fast Radio Bursts and Hubble Parameter Measurements

Yang Liu[1], Hongwei Yu[1,2], and Puxun Wu[1,2]
[1] Department of Physics and Synergistic Innovation Center for Quantum Effects and Applications, Hunan Normal University, Changsha, Hunan 410081, People's Republic of China; yangl@hunnu.edu.cn, hwyu@hunnu.edu.cn
[2] Institute of Interdisciplinary Studies, Hunan Normal University, Changsha, Hunan 410081, People's Republic of China; pxwu@hunnu.edu.cn
Received 2023 January 27; revised 2023 March 13; accepted 2023 March 21; published 2023 April 5

Abstract

We establish a cosmological-model-independent method to determine the Hubble constant H_0 from the localized fast radio bursts (FRBs) and the Hubble parameter measurements from cosmic chronometers and obtain a first such determination $H_0 = 71 \pm 3\ \mathrm{km\,s^{-1}\,Mpc^{-1}}$, with an uncertainty of 4%, from the eighteen localized FRBs and nineteen Hubble parameter measurements in the redshift range $0 < z \leqslant 0.66$. This value, which is independent of the cosmological model, is consistent with the results from the nearby Type Ia supernovae (SNe Ia) data calibrated by Cepheids and the Planck cosmic microwave background radiation observations at the 1σ and 2σ confidence level, respectively. Simulations show that the uncertainty of H_0 can be decreased to the level of that from the nearby SNe Ia when mock data from 500 localized FRBs with 50 Hubble parameter measurements in the redshift range of $0 < z \leqslant 1$ are used. Since localized FRBs are expected to be detected in large quantities, our method will be able to give a reliable and more precise determination of H_0 in the very near future, which will help us to figure out the possible origin of the Hubble constant disagreement.

Unified Astronomy Thesaurus concepts: Cosmology (343)

1. Introduction

The cosmological constant Λ plus cold dark matter (ΛCDM) model is the simplest cosmological model, which fits the observational data very well. Based on the ΛCDM model, the Planck Cosmic Microwave Background (CMB) radiation observations give a tight constraint on the Hubble constant H_0: $H_0 = 67.4 \pm 0.5\ \mathrm{km\,s^{-1}\,Mpc^{-1}}$ with an uncertainty of about 0.7% (Planck Collaboration 2020). This result, however, has a more than 5σ deviation from $H_0 = 73.04 \pm 1.04\ \mathrm{km\,s^{-1}\,Mpc^{-1}}$ with the uncertainty being about 1.42%, which is determined by the nearby Type Ia supernovae (SNe Ia) calibrated by Cepheids (Riess et al. 2022). Since these SNe Ia, which are calibrated by using the distance ladder, are located in a very low-redshift region, the H_0 determined with them can be regarded as almost cosmological model independent. The disagreement of H_0 between two different observations has become the most serious crisis in modern cosmology (Riess 2020; Dainotti et al. 2021; Di Valentino et al. 2021; Dainotti et al. 2022; Perivolaropoulos & Skara 2022), and it indicates that the assumed ΛCDM model used to determine the Hubble constant may be inconsistent with our present universe or there may be potentially unknown systematic errors in the observational data. It is worth noting, however, that several studies have not found any systematics that could explain the discrepancy (Efstathiou 2014; Riess et al. 2016; Cardona et al. 2017; Zhang et al. 2017; Riess et al. 2018a, 2018b; Feeney et al. 2018; Follin & Knox 2018). To precisely identify the possible origin of the H_0 disagreement, many other observational data are needed to constrain the Hubble constant. However, constraints from the vast majority of data usually depend on a presumed cosmological model.

Undoubtedly, a cosmological-model-independent determination of the Hubble constant from observational data with a redshift region larger than that of the nearby SNe Ia may shed light on the possible origin of the H_0 disagreement. In this Letter, we propose a cosmological-model-independent method to determine the value of H_0 from fast radio bursts (FRBs) and the Hubble parameter $H(z)$ measurements from cosmic chronometers and present a first determination of H_0 with such current observational data that are independent of the cosmological model, i.e., H_0 ($H_0 = 71 \pm 3\ \mathrm{km\,s^{-1}\,Mpc^{-1}}$). Considering that a huge number of FRBs will be detected in the near future, as more than one thousand FRB events are expected very day (Xiao et al. 2021), we expect to be able to achieve the precision of H_0 determination at the level from nearby SNe Ia with our method very soon.

FRBs are a type of frequently and mysteriously transient signal of millisecond duration with typical radiation frequency of ∼GHz (Lorimer et al. 2007; Petroff et al. 2019; Zhang 2020; CHIME/FRB Collaboration 2021; Zhang 2022). These signals are significantly dispersed by the ionized medium distributed along the path between the sources and the observer. The observed dispersion, quantified by the dispersion measure (DM), results mainly from the electromagnetic interaction between the signals and the free electrons in the intergalactic medium (IGM). Since the effects of the free electrons on the signals are cumulative with the increase of traveling distance of FRBs, the DM-redshift relations of FRBs can be used for cosmological purposes. For example, they have been used to determine the fraction of baryon mass in the IGM (Li et al. 2019; Wei et al. 2019; Li et al. 2020; Lemos et al. 2022) to constrain the cosmological parameters (Gao et al. 2014; Yang & Zhang 2016; Walters et al. 2018), to explore the reionization history of our universe (Caleb et al. 2019; Linder 2020; Beniamini et al. 2021; Bhattacharya et al. 2021; Hashimoto et al. 2021; Lau et al. 2021; Pagano & Fronenberg 2021; Heimersheim et al. 2022), to measure the Hubble parameter

(Wu et al. 2020), to probe the interaction between dark energy and dark matter (Zhao 2022), and so on.

FRBs have also been used to determine the value of the Hubble constant (Li et al. 2018; Zhao et al. 2021; Hagstotz et al. 2022; James et al. 2022; Wu & Zhang 2022; Zhao et al. 2022). Hagstotz et al. (2022) and Wu & Zhang (2022) have obtained constraints on H_0 of $62.3 \pm 9.1\ \mathrm{km\ s^{-1}\ Mpc^{-1}}$ and $68.81^{+4.99}_{-4.33}\ \mathrm{km\ s^{-1}\ Mpc^{-1}}$ by utilizing nine and eighteen localized FRBs, respectively. Using sixteen localized FRBs and sixty unlocalized FRBs, James et al. (2022) have achieved $H_0 = 73^{+12}_{-8}\ \mathrm{km\ s^{-1}\ Mpc^{-1}}$. These results rely unavoidably on an assumed cosmological model, usually ΛCDM, since the theoretical value of DM used in these studies is model dependent. Interestingly, the derivative of DM with respect to the cosmic time t is not dependent on any cosmological models although DM is, and moreover, it is proportional to the Hubble constant squared. Therefore, the value of H_0 can be determined cosmological-model-independently if the time variation of DM can be observed directly. However, the time variation of DM due to the cosmic expansion is extremely weak, which is about $-5.6 \times 10^{-8}(1+z)^2 \mathrm{pc/cm^3\ yr^{-1}}$ with z being the redshift (Yang & Zhang 2017), and thus it is very difficult to measure directly. In this Letter, we find a subtle way to avoid this problem so as to obtain H_0 cosmological-model-independently with FRBs, i.e., we propose to derive the time variation of DM through combining the redshift variation of the DM of FRBs, which can be derived from the redshift distribution of FRBs, and the Hubble parameter measurements. Since the FRB and Hubble parameter data can be in the higher-redshift region, our method contrasts with those using local measurements such as the Cepheid-calibrated SNe Ia, which can only be performed at very low redshifts.

2. Method

As is well known, the radio pulse will be dispersed when it travels through the ionized IGM, which will result in different arrival times for photons with different frequencies. For two photons with the frequencies being ν_1 and ν_2 ($\nu_1 < \nu_2$), respectively, the delayed arrival time can be expressed as

$$\Delta t = \frac{e^2}{2\pi m_e c}\left(\frac{1}{\nu_1^2} - \frac{1}{\nu_2^2}\right)\mathrm{DM}, \tag{1}$$

where e and m_e are the electron charge and mass, respectively; c is the speed of light; and DM is defined as

$$\mathrm{DM} \equiv \int \frac{n_{e,z}}{1+z} dl. \tag{2}$$

Here dl is an infinitesimal proper length along the line of sight, and $n_{e,z}$ is the number density of free electrons at redshift z. Therefore, the DM carries the information of the distance and number density of free electrons. The observed DM is a combination of four different components:

$$\mathrm{DM_{obs}} = \mathrm{DM_{MW}^{ISM}} + \mathrm{DM_{MW}^{halo}} + \mathrm{DM_{IGM}} + \mathrm{DM_{host}}. \tag{3}$$

Here the subscripts "MW," "IGM," and "host" represent the contributions from the Milky Way, the IGM, and the host galaxy, respectively. The superscripts "ISM" and "halo" denote the contributions from interstellar medium and halo of galaxy, respectively. Among them, $\mathrm{DM_{IGM}}$ depends on the cosmological model. However, since the IGM is inhomogeneous, we can only derive the average of $\mathrm{DM_{IGM}}$ theoretically (Deng & Zhang 2014):

$$\langle \mathrm{DM_{IGM}} \rangle = \frac{3cH_0\Omega_{b0}}{8\pi G m_p}\int_0^z \frac{f_{\mathrm{IGM}}(z) f_e(z)(1+z)}{E(z)} dz, \tag{4}$$

where Ω_{b0}, G, m_p, and $f_{\mathrm{IGM}}(z)$ are the current baryon density parameter, the gravitational constant, the proton mass, and the fraction of baryon mass in the IGM, respectively; $E(z) = H(z)/H_0$ is the dimensionless Hubble parameter, which is given by the concrete cosmological model; and $f_e(z) = Y_{\mathrm{H}} f_{e,\mathrm{H}}(z) + \frac{1}{2} Y_{\mathrm{He}} f_{e,\mathrm{He}}(z)$ is the ratio of the number of free electrons to baryons in the IGM. Here $Y_{\mathrm{H}} \sim 3/4$ and $Y_{\mathrm{He}} \sim 1/4$ are the hydrogen (H) and helium (He) mass fractions, respectively, and $f_{e,\mathrm{H}}$ and $f_{e,\mathrm{He}}$ are the ionization fractions for H and He, respectively.

It is worth noting that $\langle \mathrm{DM_{IGM}} \rangle$ is evolving with the cosmic expansion. After applying the relation $dz = -H_0 E(z)(1+z)dt$, we obtain the derivative of $\langle \mathrm{DM_{IGM}} \rangle$ with respect to the cosmic time t

$$\frac{d\langle \mathrm{DM_{IGM}} \rangle}{dt} = -\frac{3cH_0^2\Omega_{b0}}{8\pi G m_p} f_{\mathrm{IGM}}(z) f_e(z)(1+z)^2, \tag{5}$$

which indicates that the variation of $\langle \mathrm{DM_{IGM}} \rangle$ with time is independent of the dimensionless Hubble parameter $E(z)$ and thus of any cosmological models. As a result, the value of the Hubble constant can be derived cosmological-model-independently from

$$H_0 = \left[-\frac{8\pi G m_p}{3c\Omega_{b0} f_{\mathrm{IGM}}(z) f_e(z)(1+z)^2}\frac{d\langle \mathrm{DM_{IGM}} \rangle}{dt}\right]^{\frac{1}{2}} \tag{6}$$

if one can obtain $d\langle \mathrm{DM_{IGM}} \rangle/dt$ and fix Ω_{b0}, $f_{\mathrm{IGM}}(z)$, and $f_e(z)$. Since the variation of $\langle \mathrm{DM_{IGM}} \rangle$ from cosmic expansion is about $-5.6 \times 10^{-8}(1+z)^2\ \mathrm{pc/cm^3/yr}$ (Yang & Zhang 2017), it is extremely weak and thus is very difficult to measure. Fortunately, $d\langle \mathrm{DM_{IGM}} \rangle/dt$ can be obtained as a product of $d\langle \mathrm{DM_{IGM}} \rangle/dz$ and dz/dt. The variation of $\langle \mathrm{DM_{IGM}} \rangle$ with time can be determined once both $d\langle \mathrm{DM_{IGM}} \rangle/dz$ and dz/dt are known. The dz/dt factor can be found directly from the Hubble parameter measurements from cosmic chronometers. If we work out the relation of $\langle \mathrm{DM_{IGM}} \rangle$ with z from the observational data of FRBs, $d\langle \mathrm{DM_{IGM}} \rangle/dz$ at the redshifts of the Hubble parameter data points can be derived, and then $d\langle \mathrm{DM_{IGM}} \rangle/dt$ at the same redshifts can be obtained. For example, employing a continuous piecewise linear function to approximate the $\langle \mathrm{DM_{IGM}} \rangle - z$ relation, we have

$$\langle \mathrm{DM_{IGM}} \rangle(z) = \frac{\langle \mathrm{DM_{IGM}} \rangle_{i+1} - \langle \mathrm{DM_{IGM}} \rangle_i}{z_{i+1} - z_i}(z - z_i) + \langle \mathrm{DM_{IGM}} \tag{7}$$

after dividing uniformly the redshift range of FRB samples into n bins with $n+1$ control points z_i. Here $\langle \mathrm{DM_{IGM}} \rangle_i$ is the undetermined DM at z_i, and $z_1 = 0$ is fixed. For the $n = 1$ case, this function reduces to a linear function, and z_2 is the maximum redshift of FRB samples. Thus, we can fix $\langle \mathrm{DM_{IGM}} \rangle_1 = 0$ and obtain $\langle \mathrm{DM_{IGM}} \rangle_2$ from the observed $\langle \mathrm{DM_{IGM}} \rangle$ by using the Markov Chain Monte Carlo (MCMC) method. Taking the derivative of Equation (7) with respect to z

yields the $d\langle \mathrm{DM_{IGM}}\rangle/dz - z$ relation, from which the values of $d\langle \mathrm{DM_{IGM}}\rangle/dt$ at the redshifts of the Hubble parameter measurements can be obtained after using the $H(z)$ data. Therefore, using Equation (6), we can constrain the Hubble constant.

3. Data and Results

We will use the latest localized FRBs data and the $H(z)$ data to determine $d\langle \mathrm{DM_{IGM}}\rangle/dt$. Our FRB samples are compiled in Wu & Zhang (2022), which contain eighteen FRBs within the redshift range of $z \in (0, 0.66]$ (Chatterjee et al. 2017; Prochaska et al. 2019a; Bannister et al. 2019; Ravi et al. 2019; Bhandari et al. 2020; Heintz et al. 2020; Law et al. 2020; Marcote et al. 2020; Bhardwaj et al. 2021; Chittidi et al. 2021; Bhandari et al. 2022). The number of the latest $H(z)$ data is 32, spanning redshifts from 0.07 to 1.965 (Simon et al. 2005; Stern et al. 2010; Moresco et al. 2012; Cong et al. 2014; Moresco 2015; Moresco et al. 2016; Ratsimbazafy et al. 2017; Borghi et al. 2022), which are measured by using the cosmic chronometric technique (Jimenez & Loeb 2002). Here we select only nineteen $H(z)$ data that fall in the redshift range of the FRB samples.

Since $\mathrm{DM_{obs}}$ is released for the FRB data, we use Equation (3) to extract the extragalactic DM by deducting the contribution from the Milky Way in $\mathrm{DM_{obs}}$:

$$\mathrm{DM_{ext}^{obs}} = \mathrm{DM_{obs}} - \mathrm{DM_{MW}^{ISM}} - \mathrm{DM_{MW}^{halo}} - \Delta\mathrm{DM_{IGM}}, \quad (8)$$

where $\Delta\mathrm{DM_{IGM}}$ represents the contribution of fluctuations of the electron density in the IGM, which is assumed to obey a normal distribution $\mathcal{N}(0, \sigma_{\Delta\mathrm{DM_{IGM}}})$ since the fluctuations in the electron density along the line of sight can be approximated by a Gaussian distribution (Jaroszynski 2019; Macquart et al. 2020; Zhang et al. 2021). The $\mathrm{DM_{MW}^{ISM}}$ can be obtained from the current electron-density model of the Milky Way (Yao et al. 2017) and $\mathrm{DM_{MW}^{halo}}$ is assumed as $65\,\mathrm{pc\,cm^{-3}}$ (Prochaska & Zheng 2019b). Then the uncertainty $\sigma_{\mathrm{DM_{ext}}}$ of $\mathrm{DM_{ext}^{obs}}$ has the form

$$\sigma_{\mathrm{DM_{ext}}}^2 = \sigma_{\mathrm{DM_{obs}}}^2 + \sigma_{\mathrm{DM_{MW}}}^2 + \sigma_{\Delta\mathrm{DM_{IGM}}}^2. \quad (9)$$

Here $\sigma_{\mathrm{DM_{obs}}}$ is given by the observation; $\sigma_{\Delta\mathrm{DM_{IGM}}}$ is the uncertainty of $\Delta\mathrm{DM_{IGM}}$, which is estimated through the approximation $\sigma_{\Delta\mathrm{DM_{IGM}}}/\langle \mathrm{DM_{IGM}}\rangle = 20\%/\sqrt{z}$ given in Kumar & Linder (2019); and the uncertainty of $\mathrm{DM_{MW}}$ (containing the uncertainties of ISM and halo) is taken to be $54\,\mathrm{pc/cm^3}$ (Heimersheim et al. 2022). Apparently, the theoretical value of $\mathrm{DM_{ext}}$ can be expressed as

$$\mathrm{DM_{ext}^{\mathit{th}}} = \langle \mathrm{DM_{IGM}}\rangle + \mathrm{DM_{host}}. \quad (10)$$

However, the contribution of the host galaxy ($\mathrm{DM_{host}}$) in Equation (10) is not easy to determine since we do not know it very well. Here, we follow Macquart et al. (2020) and Zhang et al. (2020) to consider a prior log-normal distribution of $\mathrm{DM_{host}}$

$$P_{\mathrm{host}}(\mathrm{DM_{host}}) = \frac{1}{\sqrt{2\pi\sigma^2}\,\mathrm{DM_{host}}} \exp\left[-\frac{(\ln\mathrm{DM_{host}} - \mu)}{2\sigma^2}\right]. \quad (11)$$

For this log-normal distribution, the median and variance of $\mathrm{DM_{host}}$ are e^{μ} and $e^{2\mu+\sigma^2}(e^{\sigma^2} - 1)$, respectively. In Zhang et al. (2020), the value of the median e^{μ} is assumed to be redshift evolutionary: $e^{\mu} \equiv A(1+z)^{\alpha}$ with A and α being two constants. Once the allowed regions of A and α are determined from $\mathrm{DM_{ext}^{obs}}$, their best fitting values and uncertainties give the median and variation of $\mathrm{DM_{host}}$, respectively. Before running the MCMC to constrain all free parameters, we need to set the prior regions of A and α, which are obtained by using the IllustrisTNG simulation (Zhang et al. 2020). Moreover, as what was done in Zhang et al. (2020), we place the host galaxies of the FRBs into three types: (I) The repeating FRBs in a dwarf galaxy like the FRB 121102, (II) the repeating FRBs in a spiral galaxy like the FRB 180916, and (III) the nonrepeating FRBs. Thus, we set $\{A_1, \alpha_1, A_2, \alpha_2, A_3, \alpha_3\}$ as free parameters to describe the values of $\mathrm{DM_{host}}$ of FRBs in Equation (10). These six parameters will be fitted simultaneously with the coefficients in Equation (7) and are marginalized in the subsequent analysis.

For the piecewise linear function with $n = 1$, we obtain $\langle \mathrm{DM_{IGM}}\rangle_2 = 641^{+144}_{-154}\,\mathrm{pc/cm^3}$ from the eighteen FRB data points. Figure 1 shows the approximate $\langle \mathrm{DM_{IGM}}\rangle - z$ relation. Combining nineteen Hubble parameter data with the values of $d\langle \mathrm{DM_{IGM}}\rangle/dz$ at the redshifts of the $H(z)$ data, we obtain nineteen $d\langle \mathrm{DM_{IGM}}\rangle/dt$ data points. To further calculate the value of H_0, we fix $\Omega_{b0} = 0.0487 \pm 0.0005$ (DES Collaboration 2022). Due to the lack of evidence for the evolution of f_{IGM} over the redshift range covered by the FRB sample, we adopt, in our analysis, $f_{\mathrm{IGM}}(z) = 0.84^{+0.16}_{-0.22}$, which is determined by a cosmological-insensitive method (Li et al. 2020). Since the H and He are fully ionized at $z < 3$ (Meiksin 2009; Becker et al. 2011), i.e., $f_{e,\mathrm{H}} = f_{e,\mathrm{He}} = 1$, we set $f_e(z) = 7/8$ in our analysis. Finally, nineteen H_0 are derived from Equation (6). Using the minimum χ^2 method, we arrive at a constraint on H_0: $H_0 = 71 \pm 3\,\mathrm{km\,s^{-1}\,Mpc^{-1}}$ with an uncertainty of 4%. Figure 2 shows a comparison between our result with those obtained by the Planck CMB observations (Planck Collaboration 2020) and the nearby SNe Ia data (Riess et al. 2022). Our result is consistent with that from nearby SNe Ia at the 1σ confidence level (CL) but with that from the CMB observations only at the 2σ CL.

Since $\Omega_{b0} = 0.0487 \pm 0.0005$ (DES Collaboration 2022), which is used in the above analysis, depends on the ΛCDM model, to study the effect of this model-dependent value on our result, we also consider $\Omega_{b0} = 0.048 \pm 0.001$ from the wCDM model (DES Collaboration 2022) and obtain $H_0 = 71 \pm 3\,\mathrm{km\,s^{-1}\,Mpc^{-1}}$. This result is very consistent with that in the case of $\Omega_{b0} = 0.0487 \pm 0.0005$. To further investigate the effect of the uncertainty of Ω_{b0} on our result, we choose a value of Ω_{b0} with a larger uncertainty: $\Omega_{b0} = 0.0487 \pm 0.02$ and achieve $H_0 = 71 \pm 5\,\mathrm{km\,s^{-1}\,Mpc^{-1}}$ with 7% uncertainty. Apparently, when the uncertainty of Ω_{b0} increases 40 times (from 0.0005 to 0.02), the uncertainty of H_0 only increases 3%, which indicates that the precision of H_0 does not depend sensitively on the uncertainty of Ω_{b0}. Thus, we conclude that the value of H_0 from our method is insensitive to Ω_{b0}.

Let us now examine whether the adoption of the $n = 1$ piecewise linear function leads to some bias in our results. For this purpose, we perform a further analysis by using the $n = 2$ piecewise linear function and the quadratic polynomial function

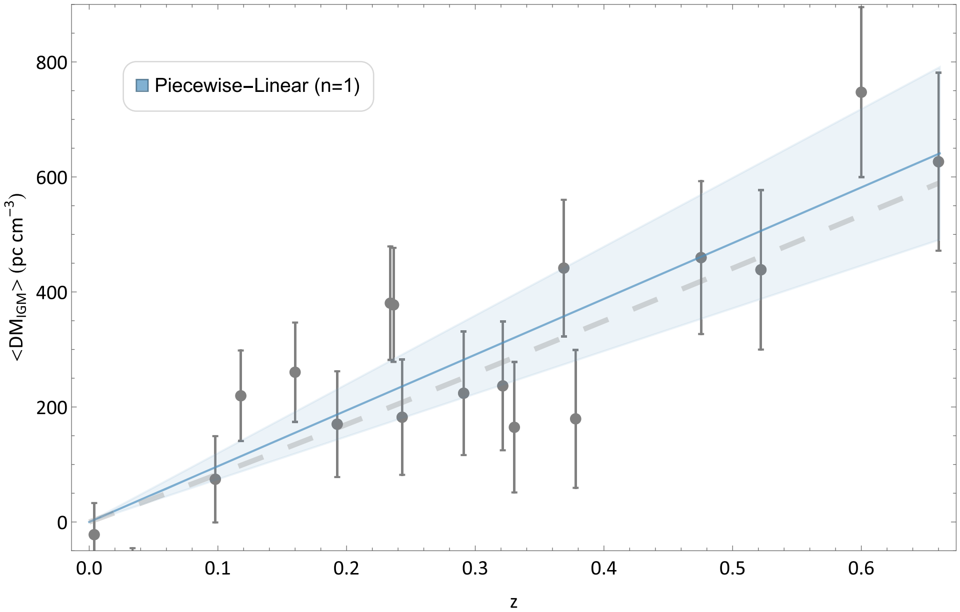

Figure 1. The $\langle \mathrm{DM_{IGM}} \rangle - z$ relation for the $n = 1$ piecewise linear function (blue line). The shadow region denotes the 1σ uncertainty. The gray points are eighteen $\langle \mathrm{DM_{IGM}} \rangle$ data samples. The dashed line is the theoretical value of $\langle \mathrm{DM_{IGM}} \rangle$ based on the ΛCDM model.

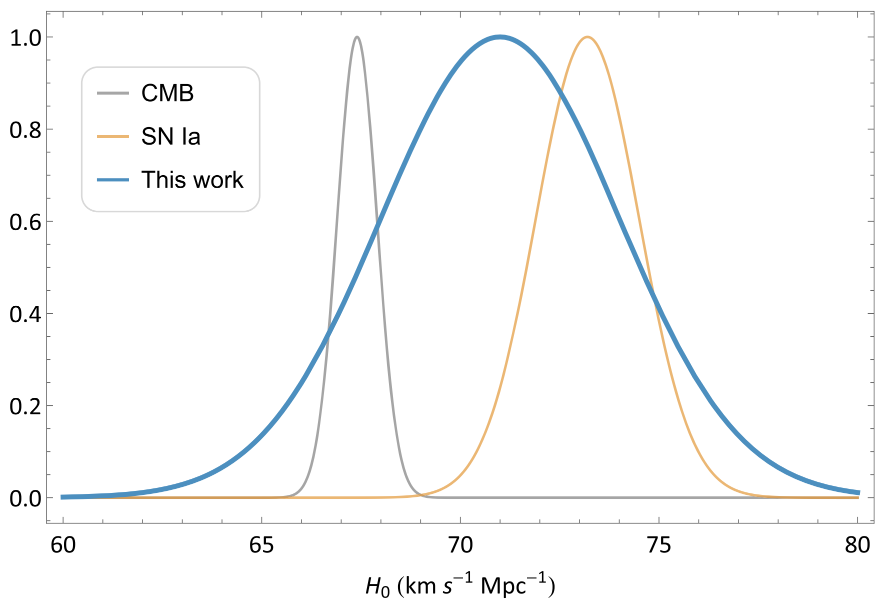

Figure 2. The constraints on H_0. The gray and orange lines represent the results from the Planck CMB observations and the nearby SNe Ia data, respectively. The blue line shows our result.

($\langle \mathrm{DM_{IGM}} \rangle(z) = Az + Bz^2$) to approximate the $\langle \mathrm{DM_{IGM}} \rangle - z$ relation, where A and B are two constants. The constraints on the Hubble constant are $H_0 = 71 \pm 5\ \mathrm{km\ s^{-1}\ Mpc^{-1}}$ and $H_0 = 71 \pm 4\ \mathrm{km\ s^{-1}\ Mpc^{-1}}$ for the $n = 2$ piecewise linear function and the quadratic polynomial, respectively. Apparently, the constraints on H_0 are very consistent with each other for three different approximations. Thus, we can conclude that the H_0 results are almost independent of the functions chosen to approximate the redshift evolution of $\langle \mathrm{DM_{IGM}} \rangle(z)$.

Let us note that our results are slightly tighter than $H_0 = 75.7^{+4.5}_{-4.4}\ \mathrm{km\ s^{-1}\ Mpc^{-1}}$ obtained model-independently from four strong gravitational lensing systems and SNe Ia (Collett et al. 2019), which is later improved to $H_0 = 72.8^{+1.6}_{-1.7}\ \mathrm{km\ s^{-1}\ Mpc^{-1}}$ when six strong gravitational lensing systems are used (Liao et al. 2020). These cosmological-model-independent results from strong lensing systems and SNe Ia are consistent with $72.5^{+2.1}_{-2.3}\ \mathrm{km\ s^{-1}\ Mpc^{-1}}$ (Birrer et al. 2019) and $73.3^{+1.7}_{-1.8}\ \mathrm{km\ s^{-1}\ Mpc^{-1}}$ (Wong et al. 2020) obtained before from the four and six lensing systems, respectively, with an assumed spatially flat ΛCDM model. Furthermore, simulations show that 400 lensing systems can constrain H_0 model-independently with an uncertainty at the level of nearby SNe Ia (Collett et al. 2019).

To see how many FRBs are needed for a determination H_0 as precise as of the level of the nearby SNe Ia, we need to use the Monte Carlo simulation. During simulation, we choose the spatially flat ΛCDM model with $H_0 = 73.04\ \mathrm{km\ s^{-1}\ Mpc^{-1}}$ and $\Omega_{m0} = 0.3$ to be the fiducial model and set $\Omega_{b0} = 0.0487$, $f_{\mathrm{IGM}} = 0.84$, and $f_e(z) = 7/8$. Here we randomly sample $\mathrm{DM_{ext}^{sim}}$ as the observed quantity, which is obtained from

$\mathrm{DM}_{\mathrm{IGM}}^{\mathrm{sim}} + \mathrm{DM}_{\mathrm{host}}^{\mathrm{sim}}$. The redshift distribution of FRBs is assumed to be $P(z) \propto z^2 \exp(-7z)$ in the redshift range $0 < z \leqslant 1$ (Hagstotz et al. 2022). At the mock redshift z, the fiducial value of $\langle \mathrm{DM}_{\mathrm{IGM}}^{\mathrm{fid}} \rangle$ can be calculated from Equation (4). The $\mathrm{DM}_{\mathrm{IGM}}^{\mathrm{sim}}$ is sampled from $\mathcal{N}(\langle \mathrm{DM}_{\mathrm{IGM}}^{\mathrm{fid}} \rangle, \sigma_{\Delta \mathrm{DM}_{\mathrm{IGM}}})$ with $\sigma_{\Delta \mathrm{DM}_{\mathrm{IGM}}} = 20\% \langle \mathrm{DM}_{\mathrm{IGM}}^{\mathrm{fid}} \rangle / \sqrt{z}$ (Kumar & Linder 2019). $\mathrm{DM}_{\mathrm{host}}^{\mathrm{sim}}$ is simulated by using the distribution $P_{\mathrm{host}}(\mathrm{DM}_{\mathrm{host}})$ given in Equation (11). The type of the host galaxy is chosen randomly from one of the three different types, and the prior values of the parameters μ and σ are set from the IllustrisTNG simulation (Zhang et al. 2020). Meanwhile, we also sample the $H(z)$ data with a uniform distribution at $0 < z \leqslant 1$ following Ma & Zhang (2011). We simulate 500 FRBs and 50 $H(z)$ data. The larger number of data sets prompts us to use the piecewise linear function with $n = 2$ to approximate the $\langle \mathrm{DM}_{\mathrm{IGM}} \rangle - z$ relation. To minimize randomness and to ensure that the final constraint result is unbiased, we repeat the above steps 100 times and finally obtain $H_0 = 73.7 \pm 1.4\ \mathrm{km\,s^{-1}\,Mpc^{-1}}$. This indicates that the uncertainty of H_0 can be decreased to 1.9% from mock data, which is almost of the same precision as that from the nearby SNe Ia (1.42%).

A high-precision determination of H_0 from FRBs is expected soon since a large number of localized FRBs will be detected in the next few years. This is because there are huge number of FRB events every day, and the detection ability is being improved rapidly. The running and upcoming radio telescopes and surveys include the Swinburne University of Technology's digital backend for the Molonglo Observatory Synthesis Telescope array (Caleb et al. 2016), the Canadian Hydrogen Intensity Mapping Experiment (CHIME; Bandura et al. 2014; CHIME/FRB Collaboration 2021), the Hydrogen Intensity and Real-time Analysis eXperiment (Newburgh et al. 2016), the Five-hundred-meter Aperture Spherical Telescope (Li et al. 2018), and the Square Kilometre Array project (Macquart et al. 2015; Fialkov & Loeb 2017).

4. Conclusion

The disagreement between the measurements of the Hubble constant from the CMB observations and the nearby SNe Ia data has become one of the pressing challenges in modern cosmology. A cosmological-model-independent method to determine the value of H_0 from the data in the redshift region larger than that of the nearby SNe Ia may serve as a probe to the possible origin of H_0 disagreement. In this Letter, we establish a feasible way to cosmological-model-independently constrain H_0 by combining the variation of $\langle \mathrm{DM}_{\mathrm{IGM}} \rangle$ with the redshift of FRBs and the Hubble parameter measurements and obtain a first such determination $H_0 = 71 \pm 3\ \mathrm{km\,s^{-1}\,Mpc^{-1}}$ with data from the eighteen localized FRBs and nineteen Hubble parameter measurements in the redshift range $0 < z \leqslant 0.66$. Remarkably, this value, which is independent of the cosmological model, lies in the middle of the results from CMB observations and the nearby SNe Ia data, and it is consistent with those from the nearby SNe Ia data and the CMB observations at the 1σ and 2σ CL, respectively. The uncertainty of our result is much less than what was obtained from FRBs in the framework of the ΛCDM model (Hagstotz et al. 2022; Wu et al. 2022; James et al. 2022).

However, as our result has large uncertainty, it does not show significant statistic evidence for preferring the result from the nearby SNe Ia data. Through the Monte Carlo simulation, we further investigate how many FRBs and $H(z)$ measurements are needed to more precisely determine the value of H_0. We find that the uncertainty of H_0 from mock 500 localized FRBs and 50 $H(z)$ data at $0 < z \leqslant 1$ can be decreased to 1.9%, which is of the same level as that from the nearby SNe Ia data. Since localized FRBs are expected to be detected in large quantities, the method established in this paper will be able to give a reliable and more precise determination of H_0 in the very near future, which will help us to figure out the possible origin of the Hubble constant disagreement.

This work was supported in part by the NSFC under Grant Nos. 12275080, 12075084, 11805063, and 12073069.

References

Bandura, k., Addison, G. E., Amiri, M., et al. 2014, Proc. SPIE, 9145, 914522
Bannister, K. W., Deller, A. T., Phillips, C., et al. 2019, Sci, 365, 565
Becker, G. D., Bolton, J. S., Haehnelt, M. G., & Sargent, W. L. W. 2011, MNRAS, 410, 1096
Beniamini, P., Kumar, P., Ma, X., & Quataert, E. 2021, MNRAS, 502, 5134
Bhandari, S., Heintz, K. E., Aggarwal, K., et al. 2022, AJ, 163, 69
Bhandari, S., Sadler, E. M., Prochaska, J. X., et al. 2020, ApJL, 895, L37
Bhardwaj, M., Kirichenko, A. Y., Michilli, D., et al. 2021, ApJL, 919, L24
Bhattacharya, M., Kumar, P., & Linder, E. V. 2021, PhRvD, 103, 103526
Birrer, S., Treu, T., Rusu, C. E., et al. 2019, MNRAS, 484, 4726
Borghi, N., Moresco, M., & Cimatti, A. 2022, ApJL, 928, L4
Caleb, M., Flynn, C., Bailes, M., et al. 2016, MNRAS, 458, 718
Caleb, M., Flynn, C., & Stappers, B. W. 2019, MNRAS, 485, 2281
Cardona, W., Kunz, M., & Pettorino, V. 2017, JCAP, 03, 056
Chatterjee, S., Law, C. J., Wharton, R. S., et al. 2017, Natur, 541, 58
CHIME/FRB Collaboration 2021, ApJS, 257, 59
Chittidi, J., Simha, S., & Mannings, S. 2021, ApJ, 922, 173
Collett, T., Montanari, F., & Räsänen, S. 2019, PhRvL, 123, 231101
Cong, Z., Han, Z., Shuo, Y., et al. 2014, RAA, 14, 1221
Dainotti, M. G., Simone, B. D., Schiavone, T., et al. 2021, ApJ, 912, 150
Dainotti, M. G., Simone, B. D., Schiavone, T., et al. 2022, Galax, 10, 24
Deng, W., & Zhang, B. 2014, ApJL, 783, L35
DES Collaboration 2022, PhRvD, 105, 023520
Di Valentino, E., Mena, O., Pan, S., et al. 2021, CQGra, 38, 153001
Efstathiou, G. 2014, MNRAS, 400, 1138
Feeney, S. M., Mortlock, D. J., & Dalmasso, N. 2018, MNRAS, 476, 3861
Fialkov, A., & Loeb, A. 2017, ApJL, 846, L27
Follin, B., & Knox, L. 2018, MNRAS, 477, 4534
Gao, H., Li, Z., & Zhang, B. 2014, ApJ, 788, 189
Hagstotz, S., Reischke, R., & Lilow, R. 2022, MNRAS, 511, 662
Hashimoto, T., Goto, T., Lu, T.-Y., et al. 2021, MNRAS, 502, 2346
Heimersheim, S., Sartorio, N. S., Fialkov, A., & Lorimer, D. R. 2022, ApJ, 933, 57
Heintz, K. E., Prochaska, J. X., Simha, S., et al. 2020, ApJ, 903, 152
James, C. W., Ghosh, E. M., Prochaska, J. X., et al. 2022, MNRAS, 516, 4862
Jaroszynski, M. 2019, MNRAS, 484, 1637
Jimenez, R., & Loeb, A. 2002, ApJ, 573, 37
Kumar, P., & Linder, E. V. 2019, PhRvD, 100, 083533
Lau, A. W. K., Mitra, A., Shafiee, M., & Smoot, G. 2021, NewA, 89, 101627
Law, C. J., Butler, B. J., Prochaska, J. X., et al. 2020, ApJ, 899, 161
Lemos, T., Gonçalves, R. S., Carvalho, J. C., & Alcaniz, J. S. 2023, EPJC, 83, 138
Li, D., Wang, P., Qian, L., et al. 2018, IMMag, 19, 112
Li, Z., Gao, H., Wei, J.-J., et al. 2019, ApJ, 876, 146
Li, Z., Gao, H., Wei, J.-J., et al. 2020, MNRASLett., 496, L28
Li, Z.-X., Gao, H., Ding, X.-H., Wang, G.-J., & Zhang, B. 2018, NatCo, 9, 3833
Liao, K., Shafieloo, A., Keeley, R. E., & Linder, E. V. 2020, ApJL, 895, L29
Linder, E. V. 2020, PhRvD, 101, 103019
Lorimer, D. R., Bailes, M., McLaughlin, M. A., Narkevic, D. J., & Crawford, F. 2007, Sci, 318, 777
Ma, C., & Zhang, T.-J. 2011, ApJ, 730, 74
Macquart, J.-P., Keane, E., Grainge, K., et al. 2015, in Proc. of Advancing Astrophysics with the Square Kilometre Array (AASKA14)in Proceedings of Advancing Astrophysics with the Square Kilometre Array (AASKA14)., 55
Macquart, J. P., Prochaska, J. X., McQuinn, M., et al. 2020, Natur, 581, 391
Marcote, B., Nimmo, K., Hessels, J. W. T., et al. 2020, Natur, 577, 190

Meiksin, A. A. 2009, RvMP, 81, 1405
Moresco, M. 2015, MNRASLett., 450, L16
Moresco, M., Cimatti, A., Jimenez, R., et al. 2012, JCAP, 08, 006
Moresco, M., Pozzetti, L., Cimatti, A., et al. 2016, JCAP, 05, 014
Newburgh, L. B., Bandura, K., Bucher, M. A., et al. 2016, Proc. SPIE, 9906, 99065X
Pagano, M., & Fronenberg, H. 2021, MNRAS, 505, 2195
Perivolaropoulos, L., & Skara, F. 2022, NewAR, 95, 101659
Petroff, E., Hessels, J. W. T., & Lorimer, D. R. 2019, A&ARv, 27, 4
Planck Collaboration 2020, A&A, 641, A6
Prochaska, J. X., Macquart, J. P., & Mcquinn, M. 2019a, Sci, 366, 231
Prochaska, J. X., & Zheng, Y. 2019b, MNRAS, 485, 648
Ratsimbazafy, A. L., Loubser, S. I., Crawford, S. M., et al. 2017, MNRAS, 467, 3239
Ravi, V., Catha, M., D'Addario, L., et al. 2019, Natur, 572, 352
Riess, A. G. 2020, NatRP, 2, 10
Riess, A. G., Casertano, S., Yuan, W., et al. 2018a, ApJ, 855, 136
Riess, A. G., Casertano, S., Yuan, W., et al. 2018b, ApJ, 861, 126
Riess, A. G., Macri, L. M., Hoffmann, S. L., et al. 2016, ApJ, 826, 56
Riess, A. G., Yuan, W., Macri, L. M., et al. 2022, ApJL, 934, L7
Simon, J., Verde, L., & Jimenez, R. 2005, PhRvD, 71, 123001
Stern, D., Jimenez, R., Verde, L., Kamionkowski, M., & Stanford, S. A. 2010, JCAP, 02, 008
Walters, A., Weltman, A., Gaensler, B. M., Ma, Y.-Z., & Witzemann, A. 2018, ApJ, 856, 65
Wei, J.-J., Li, Z., Gao, H., & Wu, X.-F. 2019, JCAP, 09, 039
Wong, K. C., Suyu, S. H., & Chen, G. C. F. 2020, MNRAS, 498, 1420
Wu, Q., Yu, H., & Wang, F. Y. 2020, ApJ, 895, 33
Wu, Q., Zhang, G.-Q., & Wang, F. Y. 2022, MNRASLett., 515, L1
Xiao, D., Wang, F., & Dai, Z. 2021, SCPMA, 64, 249501
Yang, Y.-P., & Zhang, B. 2016, ApJL, 830, L31
Yang, Y.-P., & Zhang, B. 2017, ApJ, 847, 22
Yao, J. M., Manchester, R. N., & Wang, N. 2017, ApJ, 835, 29
Zhang, B. 2020, Natur, 587, 45
Zhang, B. 2022, arXiv:2212.03972
Zhang, B. R., Childress, M. J., Davis, T. M., et al. 2017, MNRAS, 471, 2254
Zhang, G. Q., Yu, H., He, J. H., & Wang, F. Y. 2020, ApJ, 900, 170
Zhang, Z. J., Yan, K., Li, C. M., Zhang, G. Q., & Wang, F. Y. 2021, ApJ, 906, 49
Zhao, S., Liu, B., Li, Z., & Gao, H. 2021, ApJ, 916, 70
Zhao, Z.-W., Wang, L.-F., Zhang, J.-G., Zhang, J.-F., & Zhang, X. 2022, arXiv:2210.07162
Zhao, Z.-W., Zhang, J.-G., Li, Y., et al. 2022, arXiv:2212.13433